



GR Letter

First documented deep submarine explosive eruptions at the Marsili Seamount (Tyrrhenian Sea, Italy): A case of historical volcanism in the Mediterranean Sea



Gianluca Iezzi ^{a,b}, Carlo Caso ^{a,c}, Guido Ventura ^{b,*}, Mattia Vallefucoco ^d, Andrea Cavallo ^b, Harald Behrens ^e, Silvio Mollo ^b, Diego Paltrinieri ^f, Patrizio Signanini ^a, Francesco Vetere ^{a,e}

^a Dipartimento di Ingegneria & Geologia, Università G. d'Annunzio, Chieti, Italy

^b Istituto Nazionale di Geofisica e Vulcanologia, Roma, Italy

^c Schlumberger Information Solutions, Madrid, Spain

^d Istituto Ambiente Marino Costiero IAMC, CNR, Napoli, Italy

^e Institute for Mineralogy, Leibniz University, Hannover, Germany

^f Eurobuilding, Servigliano (AP), Italy

ARTICLE INFO

Article history:

Received 17 July 2013

Received in revised form 7 November 2013

Accepted 7 November 2013

Available online 25 November 2013

Handling Editor: I. Safonova

Keywords:

Submarine active volcanism

Explosive eruption

Holocene tephra

Back-arc

Hazard

ABSTRACT

The Marsili Seamount (MS) is an about 3200 m high volcanic complex measuring 70 × 30 km with the top at ~500 m b.s.l. MS is interpreted as the ridge of the 2 Ma old Marsili back-arc basin belonging to the Calabrian Arc–Ionian Sea subduction system (Southern Tyrrhenian Sea, Italy). Previous studies indicate that the MS activity developed between 1 and 0.1 Ma through effusions of lava flows. Here, new stratigraphic, textural, geochemical, and ¹⁴C geochronological data from a 95 cm long gravity core (COR02) recovered at 839 m bsl in the MS central sector are presented. COR02 contains mud and two tephra consisting of 98 to 100 area% of volcanic ash. The thickness of the upper tephra (TEPH01) is 15 cm, and that of the lower tephra (TEPH02) is 60 cm. The tephra have poor to moderate sorting, loose to partly welded levels, and erosive contacts, which imply a short distance source of the pyroclastics. ¹⁴C dating on fossils above and below TEPH01 gives an age of 3 ka BP. Calculations of the sedimentation rates from the mud sediments above and between the tephra suggest that a formation of TEPH02 at 5 ka BP MS ashes has a high-K calcalkaline affinity with 53 wt.% < SiO₂ < 68 wt.%, and their composition overlaps that of the MS lava flows. The trace element pattern is consistent with fractional crystallization from a common, OIB-like basalt. The source area of ashes is the central sector of MS and not a subaerial volcano of the Campanian and/or Aeolian Quaternary volcanic districts. Submarine, explosive eruptions occurred at MS in historical times: this is the first evidence of explosive volcanic activity at a significant (500–800 m bsl) water depth in the Mediterranean Sea. MS is still active, the monitoring and an evaluation of the different types of hazards are highly recommended.

© 2013 International Association for Gondwana Research. Published by Elsevier B.V. All rights reserved.

1. Introduction

The Marsili Seamount (MS; Southern Tyrrhenian Sea, Italy) is the largest volcano of the Mediterranean area and Europe, measuring about 70 km in length and 30 km in width (Fig. 1a, b, c). MS, which is elongated in a NNE–SSW direction, rises up from the bathyal plain of the Marsili basin at 3500 up to 508 m below the sea level (bsl) (Fig. 1b, c). MS is located in the Marsili back-arc basin, to the north of the Aeolian volcanic Arc, and is associated to the subduction of the Ionian slab below the Calabrian Arc (Fig. 1a) (Malinverno and Ryan, 1986; Rosenbaum and Lister, 2004). MS is believed to represent the super-inflated ridge of the Marsili back-arc, which opened at about 2 Ma (Marani and Trua, 2002; Nicolosi et al., 2006; Cocchi et al., 2009). Recent morphological and volcanological data show, however, that MS could

represent a volcanic arc edifice emplaced on the ‘relict’ back-arc basin (Ventura et al., 2013).

The dredged lavas of MS show a calc-alkaline affinity related to IAB- and OIB-like mantle sources; these lavas range from basalts to basaltic andesites and trachyandesites (Trua et al., 2002). Basaltic lavas show low- to medium-K signatures, whereas more evolved rocks, which have been dredged only on the MS axial zone, show a medium- to high-K character (Peccerillo, 2005; Trua et al., 2005, 2011). Geophysical and geochemical data reveal that MS is affected by active degassing from a deep (mantle) source (Lupton et al., 2011), and by shallow seismicity related to volcanotectonic events and hydrothermal activity (D'Alessandro et al., 2009). Modeling of magnetic and gravity data suggests the occurrence of a magmatic reservoir within the seamount (Caratori Tontini et al., 2010). The above summarized data suggest that MS could be still active. The time evolution of the MS volcanism is barely constrained: based on magnetic data and previous age estimates, Cocchi et al. (2009) proposed that the early vertical accretion of MS started at about 1 Ma, then the growth of the edifice mainly occurred

* Corresponding author at: Istituto Nazionale di Geofisica e Vulcanologia, Via di Vigna Murata 605, 00143 Roma, Italy. Tel.: +39 06 51860221.

E-mail address: guido.ventura@ingv.it (G. Ventura).

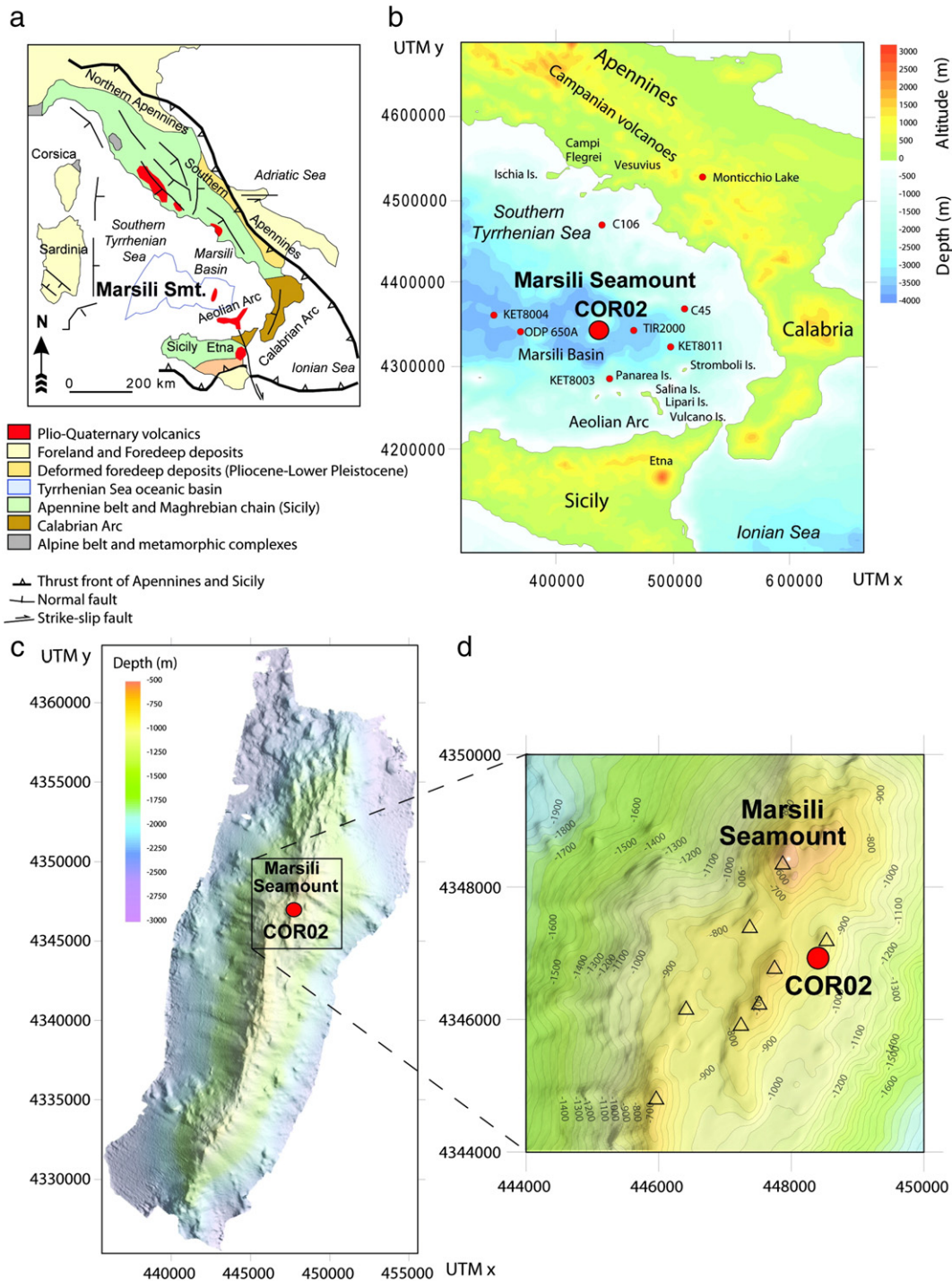


Fig. 1. (a) Geodynamic setting of the Southern Tyrrhenian Sea and location of the Marsili Seamount (modified from De Ritis et al., 2010). (b) Location of the CORE02 log (this study) on the Marsili Seamount and of the other logs (KET8003, KET8004, KET8011, ODP-650A, TIR2000, C45 and C106) in the Tyrrhenian Sea and Apennines (location from Paterne et al., 1988; Calanchi et al., 1994; Munno and Petrosino, 2004; Di Roberto et al., 2008; Wulf et al., 2008). (c) Shaded relief map of the Marsili Seamount and bathymetry (data from Ventura et al., 2013) with the location of the CORE02 log. (d) Bathymetry of the central sector of the Marsili Seamount and location of the volcanic cones (triangles; data from Ventura et al., 2013).

between 0.78 and 0.1–0.2 Ma. 0.1 Ma is assumed to be the youngest age for the MS volcanism (Selli et al., 1977; Peccerillo, 2005). On the basis of the data collected on the flanks and summit of MS, the volcanism appears to be related to effusive activity alone. However, Keller and Leiber (1974) hypothesized a possible explosive activity of the seamount on the basis of two volcanoclastic levels in the Marsili basin. Different volcanoclastic layers have been recognized in the Tyrrhenian Sea and in mainland Italy (Paterne et al., 1988; Calanchi et al., 1994; Munno and Petrosino, 2004; Wulf et al., 2004, 2008; Di Roberto et al., 2008). The characterization of these volcanoclastites is of primary importance for

the reconstruction of the activity of the Mediterranean volcanoes and for the estimate of the areal dispersion of the volcanic products.

Here, we document, for the first time, the occurrence of two tephras sampled in a ~1 m long gravity core (COR02) collected at 839 m bsl in the MS central sector (Figs. 1d and 2). These tephras consist of juvenile and pristine ashes. The stratigraphy, texture, and geochemistry of these ashes, along with radiometric age determinations on fossils hosted in the sediments are presented and discussed. Our results put new, unexpected constraints on the age and type of activity of submarine volcanoes in the Mediterranean area and the hazard implications.

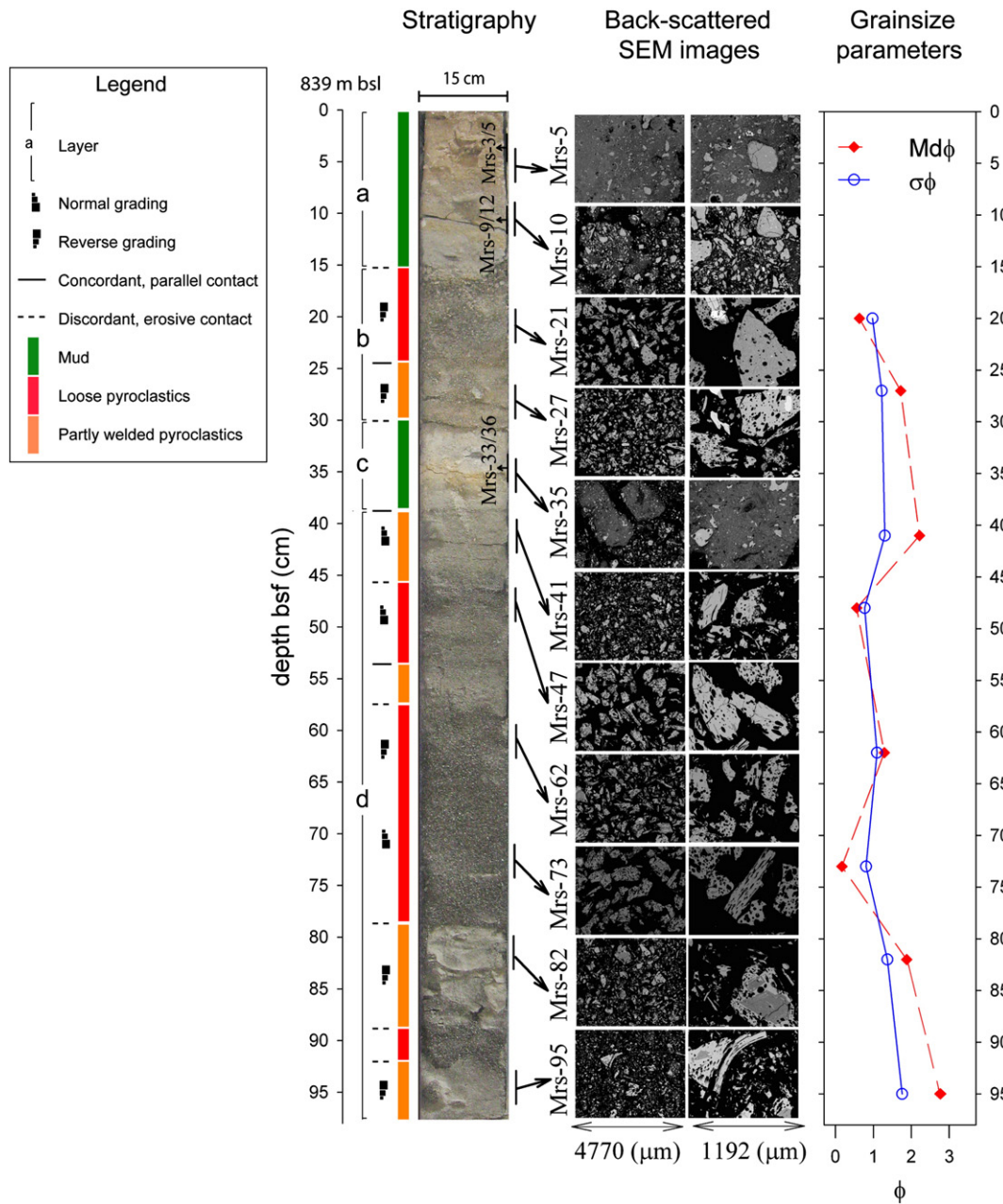


Fig. 2. Stratigraphic column of the COR02 log. The columns to the left of the log evidence the main sedimentary and volcanic layers (green = clay sediments; red = loose volcanic ash; orange = welded volcanic ash); continuous lines indicate concordant, plane-parallel surfaces, while dashed lines evidence discontinuous, erosive surfaces. The symbols of normal and reverse grading are also reported. The samples (Mrs) within the log are those selected for ^{14}C age determinations. The samples on the right of the log are those selected for image and geochemical analyses. Back-scattered SEM images at two different magnifications of each sample are also reported along with the variation of $\text{Md}\phi$ and $\sigma\phi$ with the stratigraphic height.

2. Location of the Marsili COR02 gravity core and analytical methods

The COR02 gravity core analyzed in this study was recovered at a depth of 839 m bsl during the marine cruise 'Prometheus' on board the R/V *Universitatis* in July 2006 (Caso et al., 2010). The core has coordinates UTMx 448362.45 and UTM y 4346985.26 (Zone 33; WGS84), and is positioned on the eastern boundary of a relatively flat area (slope < 5°) characterized by small (radius < 500 m, height < 250 m) cones aligned along a NNE–SSW direction (Fig. 1d). This area is located in the central sector of the seamount at about 1500 m to the south of the MS summit (508 m bsl).

The core was cut in two halves along its length and, on the basis of mesoscopic observations, eleven undisturbed samples were collected using metal spoons and knives; position and features of these samples

are reported in Table 1 and displayed in Fig. 2. The samples were embedded in epoxy resin, mounted on thin sections, and polished for back-scattered scanning electron microscopy (BS-SEM) observations using a JEOL FE-SEM6500F (INGV at Roma) equipped with an energy-dispersive spectrometer (EDS). The volcanic and sedimentary fractions of the samples were determined by image analyses on $4770 \times 3590 \mu\text{m}$ BS-SEM images, whereas the crystal, bubble and glassy fractions of the volcanic component were determined on averaging eight BS-SEM pictures with dimension $1192 \times 897 \mu\text{m}$ (100×); the image analysis procedure is detailed in Iezzi et al. (2011) and Lanzafame et al. (2013).

The chemical composition of the volcanic glass was done by an electron microprobe analysis (EPMA) JEOL-JXA8200 (INGV at Rome) equipped with a wavelength-dispersive spectrometer (WDS); the EPMA operative conditions are reported in Iezzi et al. (2008). Following

Table 1
Sample labels of the COR02 log and their stratigraphic, sedimentary, volcanic and mineralogical features.

Sample	Depth bsf (cm)	Deposit	Fossils	Ash (area%)	Md ϕ	ϕ	Bubbles (area%)	Crystals (area%)	Minerals
Mrs-5	5	Compacted mud	Present	~10			–	–	–
Mrs-10	10	Compacted mud	Present	~60			–	–	–
Mrs-21	21	Loose tephra	Absent	98	0.63	0.97	16	39	plg, cpx, sp, opx, ol, amph
Mrs-27	27	Gently welded tephra	Absent	98	1.72	1.21	13	43	plg, cpx, sp, ol, apt, mi
Mrs-35	35	Compacted mud	Present	~20			–	–	–
Mrs-41	41	Gently welded tephra	Absent	100	2.22	1.30	5	16	plg, ol, cpx, Apt
Mrs-47	47	Loose tephra	Absent	100	0.56	0.77	20	10	plg, ol, cpx
Mrs-62	62	Loose tephra	Absent	100	1.29	1.09	13	18	plg, ol, cpx, amph
Mrs-73	73	Loose tephra	Absent	100	0.17	0.81	24	11	plg, ol, cpx
Mrs-82	82	Gently welded tephra	Absent	100	1.88	1.37	8	13	plg, ol, cpx
Mrs-95	95	Gently welded tephra	Absent	98	3.04	1.76	7	14	plg, ol, cpx

Footnotes: plg: plagioclase, ol: olivine, cpx: clinopyroxene, opx: orthopyroxene, sp: spinel, amph: amphibole, mi: mica and apt: apatite. Md ϕ is the median diameter and ϕ is the sorting ($\phi = -\log_r r$, where r is the grain size in mm).

Mollo et al. (2013), the bulk tephra chemical compositions (major and trace elements; Table 2) were performed by ICP/MS using the analytical protocols “4LITHO” and “4B1” of the Activation Laboratories Ltd. (Canada).

^{14}C dating was carried out on planktonic foraminifera accurately extracted as close as possible to tephra layers from sediments in which the volcanic portions were ≤ 60 area% (Table 1). Samples 3 cm-thick were disaggregated in distilled water, wet sieved and oven dried at 50 °C. Under a binocular microscope more than 20 mg of well preserved planktonic foraminifera shells were hand-picked in the fraction 150 μm . Where possible, monospecific samples (*Globorotalia inflata*) were picked; otherwise, polyspecific assemblages were collected, in order to generate sufficient sample weight. The ^{14}C AMS measurements were performed at the AMS system installed at Centre for Isotopic Research for Cultural and Environmental heritage laboratory in Caserta (Italy) (Terrasi et al., 2007). The system is based on a tandem accelerator 9SDH-2 (built by National Electrostatics Corporation, WI, USA) with a maximum terminal voltage of 3 MV. The $\delta^{13}\text{C}$ of each sample was also measured using an elemental analyzer (ThermoFinnigan EA 1112) coupled with an IRMS (ThermoFinnigan Deltaplus) at the Department of Environmental Science (Second University of Naples, Caserta, Italy). Radiocarbon ages were calibrated using calibration software CALIB REV5.0.1 (Hughen et al., 2004). The reservoir correction DR (reservoir age) used for calibration is 400 yr (Siani et al., 2001). The calibrated age ranges are reported in years AD (BC and BP) and refer to 2 σ .

3. Results

3.1. Stratigraphy

The COR02 log consists of the following layers (from the top to the bottom; Table 1 and Fig. 2): (a) a 15 cm thick compacted muddy layer containing abundant fossils with a volcanic component (ash) between 5 and 60 area% (Mrs-5 and Mrs-10), (b) a 15 cm thick tephra (hereafter TEPH01) with only 2 area% of sediments, consisting of a loose (Mrs-21; thickness = 9 cm) to gently welded (Mrs-27; thickness = 6 cm) volcanic ash layer; (c) a muddy layer of 8 cm with > 80 area% of muddy sediments rich in fossils (Mrs-35); (d) the lowermost part of the log is constituted by a tephra (hereafter TEPH02) with a thickness of 60 cm, alternating loose (Mrs-47, Mrs-62 and Mrs-73) and gently welded (Mrs-41, Mrs-82 and Mrs-95) volcanic ashes. The contacts among the sedimentary strata and the tephtras, including the transition from loose to poorly welded ashes, are generally irregular or not planar (Fig. 2).

3.2. Texture and mineral association of tephtras

The loose portions of TEPH01 (Mrs-21) and TEPH02 (Mrs-47–62–73) are moderately sorted ($0.80 < \phi < 1.09$) (Fig. 2) with clasts of size <1 mm and Md ϕ values between 1.29 (Mrs-62) and 0.17 (Mrs-73)

(Table 1); Mrs-73 sample shows clasts with size up to 1 mm (Fig. 2). The gently welded Mrs-95 sample has the largest Md ϕ (2.77) of the log; the other three gently welded horizons (Mrs-27; Mrs-41, Mrs-82) show poor sorting ($1.21 < \phi < 1.37$) with Md ϕ between 2.22 and 1.72 (Table 1).

The ash particles of TEPH01 and TEPH02 have a low vesicularity (Fig. 2), with bubble contents between 5 and 24 area% (Table 1). Bubbles are generally unconnected and show elliptical, stretched to sub-spherical shapes (Figs. 2 and 3a, b). The ash particles are characterized by tube-like smoothed (Fig. 3a) to poorly smoothed (Fig. 3b) surfaces; minor blocky-like surfaces also occur (Fig. 3c). Pitting of finer particles and cracks is present on the surface of some clasts along with concoidal to step-like rupture surfaces (Fig. 3c, d, e). Zeolites have been also found on few clasts (Fig. 3f). Clasts from the gently welded horizons of the two tephtras have a lower amount of bubbles than that of the loose horizons (Table 1).

TEPH01 clasts have a crystal content between 39 and 43 area% with a plagioclase + clinopyroxene + olivine + spinel \pm orthopyroxene \pm amphibole \pm apatite mineral association (Table 1). TEPH02 clasts have a lower crystal content, i.e. 10 to 18 area%; the phases are: plagioclase + clinopyroxene + olivine \pm amphibole \pm apatite. Plagioclase is the most abundant phase in both tephtras.

3.3. Chemical composition of tephtras

The chemical composition of the glass matrixes and bulk samples is reported in Table 2 and displayed in Fig. 4 in the TAS (Le Bas et al., 1986) and SiO_2 vs. K_2O (Peccerillo, 2005) diagrams. The whole rock composition of TEPH01 is latitic, whereas TEPH02 is a mugearite (Fig. 4a); with the exception of the sample Mrs-95, the other samples fall in the sub-alkaline field of Irvine and Baragar (1971). The Mrs-95 sample has an abnormal amount of bulk Na_2O and LOI, which implies a contamination by some amount of marine brines. TEPH01 and TEPH02 samples fall in the field of high-K calcalkaline rocks (Fig. 4b). The glassy matrix of TEPH01 is trachytic in composition, whereas the TEPH02 ash is mugearitic to benmoreitic in composition (Fig. 4c). Both TEPH01 and TEPH02 glasses have a sub-alkaline affinity. A variation of selected major and trace elements with SiO_2 and the trace element pattern of the less evolved TEPH02 samples are reported in Figs. 5 and 6, respectively. These plots are discussed in Section 4.1.

3.4. Radiometric age determination

^{14}C dating was carried out on planktonic foraminifera from three samples located at 3 to 5 cm from the top of the log (sample Mrs-3/5), 9 to 12 cm from the top (sample Mrs-9/12), and 33 to 36 cm from top (Mrs-33/36) (Fig. 2). The samples Mrs-3/5 and Mrs-9/12 are representative of the top and bottom of the muddy layer above TEPH01, whereas the sample Mrs-33/36 is representative of the muddy level between TEPH01 and TEPH02. The obtained calibrated ages are: 264–507 A.D.

Table 2
Average oxide compositions (wt.%) of bulk and glass samples of tephras from the COR02 log, and trace element content of the bulk samples.

Sample	Mrs 21		Mrs-27		Mrs 41		Mrs-47		Mrs 62		Mrs-73		Mrs 82		Mrs-95	
	Bulk	Glass	Bulk	Glass	Bulk	Glass	Bulk	Glass	Bulk	Glass	Bulk	Glass	Bulk	Glass	Bulk	Glass
SiO ₂	60.03	62.26	61.28	63.22	53.86	55.31	54.53	55.19	54.94	56.57	54.24	55.68	55.44	56.52	53.62	56.56
TiO ₂	0.88	1.03	0.85	0.98	1.21	1.35	1.19	1.32	1.23	1.27	1.21	1.28	1.17	1.25	1.1	1.28
Al ₂ O ₃	16.58	16.3	15.59	16.41	16.66	15.63	16.64	16.29	17.01	16.27	16.17	16.47	16.78	16.38	16.14	15.93
FeO	5.79	4.71	4.8	4.39	7.61	7.47	7.41	7.29	7.41	7.72	7.88	7.82	7.16	7.41	6.78	6.98
MnO	0.13	0.13	0.12	0.11	0.15	0.14	0.14	0.15	0.15	0.16	0.15	0.15	0.14	0.15	0.13	0.15
MgO	2.25	1.73	1.8	1.53	4.15	3.7	3.9	3.74	3.99	3.75	3.86	3.94	3.63	3.61	3.49	3.57
CaO	4.15	3.72	4.07	3.49	7.81	7.02	7.91	7.34	7.53	6.93	7.97	7.35	7.2	6.76	7.28	6.86
Na ₂ O	4.81	4.64	4.41	4.79	4.44	4.09	4.16	4.07	4.25	4.17	4.04	4.06	4.73	4.26	5.77	4.23
K ₂ O	3.18	3.51	2.98	3.37	1.79	2.02	1.78	1.87	1.96	2.06	1.72	1.91	2.07	2.07	1.9	2.05
P ₂ O ₅	0.31	0.27	0.33	0.26	0.43	0.5	0.45	0.47	0.44	0.51	0.49	0.5	0.42	0.51	0.45	0.48
Cl	–	0.28	–	0.28	–	0.17	–	0.16	–	0.17	–	0.17	–	0.18	–	0.18
Total	98.7	98.58	96.8	98.82	99	97.4	98.8	98.01	100.2	99.57	98.6	99.33	99.5	99.11	97.4	98.27
S	0.2	–	0.18	–	0.1	–	0.05	–	0	–	0.04	–	0.05	–	0.1	–
LOI	2.09	–	2.92	–	1.51	–	1.35	–	0.59	–	1.03	–	1.27	–	3.46	–
H ₂ O	–	0.97	–	0.87	–	0.78	–	0.95	–	0.57	–	0.5	–	0.53	–	0.59
Alkalis	7.99	8.15	7.39	8.16	6.23	6.11	5.94	5.94	6.21	6.23	5.76	5.97	6.8	6.33	7.67	6.28
TAS	Latite	Trachyte	Latite	Trachyte	Mugearite	Mugearite	Mugearite	Mugearite	Mugearite	Mugearite	Mugearite	Mugearite	Mugearite	Mugearite	Mugearite	Mugearite
Sc	13		12		25		25		24		23		21		27	
V	112		105		255		265		272		243		234		257	
Cr	<20		<20		<20		<20		<20		<20		<20		2.8	
Co	10		9		21		22		21		20		18			
Ni	11		9		16		13		19		11		12		17	
Rb	81		92		49		49		51		51		52		2.7	
Sr	346		332		446		445		440		451		443		263	
Y	28		29		24		24		26		24		23		23	
Zr	194		218		146		131		131		145		141		17	
Nb	27		36		23		23		26		25		27		2.5	
Cs	3.8		4.4		2		2		2.2		1.9					
Ba	1318		1329		634		637		603		677		639		65	
La	40.9		57.3		34.4		34.6		40		36.6		40.5		5.6	
Ce	72.4		109		61.8		61.2		73.7		63.8		73.1		12	
Pr	7.84		11.8		7.17		6.81		8.01		6.96		7.65		1.7	
Nd	28.6		42.8		27.3		25.8		29.4		26.1		27.8		7.9	
Sm	5.6		7.6		5.4		5.1		5.6		5		5.3		2.4	
Eu	1.46		1.9		1.52		1.44		1.59		1.36		1.49		0.8	
Gd	4.8		6.2		4.7		4.6		5.1		4.3		4.6		3	
Tb	0.8		0.9		0.8		0.7		0.8		0.7		0.7		0.57	
Dy	4.6		5.4		4.5		4.2		4.7		4.1		4.3		3.8	
Ho	0.9		1.1		0.9		0.8		0.9		0.8		0.9		0.8	
Er	2.8		3.1		2.6		2.5		2.7		2.4		2.5		2.35	
Tm	0.43		0.48		0.41		0.39		0.4		0.38		0.38		0.4	
Yb	3.1		3.2		2.9		2.7		2.6		2.6		2.4		2.27	
Lu	0.54		0.54		0.47		0.44		0.43		0.43		0.41		0.34	
Hf	4.1		4.7		3.2		3		2.9		3.1		3		0.7	
Ta	1.7		2		1.4		1.3		1.4		1.5		1.6		0.17	
Pb	39		62		8		18		7		8		9		1.2	
Th	14		19.8		8.2		8.5		9.6		9.1		10.1		0.8	
U	4.2		5.9		2.3		2.3		2.7		2.5		3.1		0.3	

Footnotes: The bulk and glass compositions of TEPH01 (Mrs-21 and Mrs-27) are latite and trachyte since $\text{Na}_2\text{O}-2 < \text{K}_2\text{O}$, whereas the bulk and glass compositions for TEPH02 (Mrs-41, Mrs-47, Mrs-62) are mugearite since $\text{Na}_2\text{O}-2 > \text{K}_2\text{O}$. LOI = Loss Of Ignition. TAS = Total Alkali versus Silica.

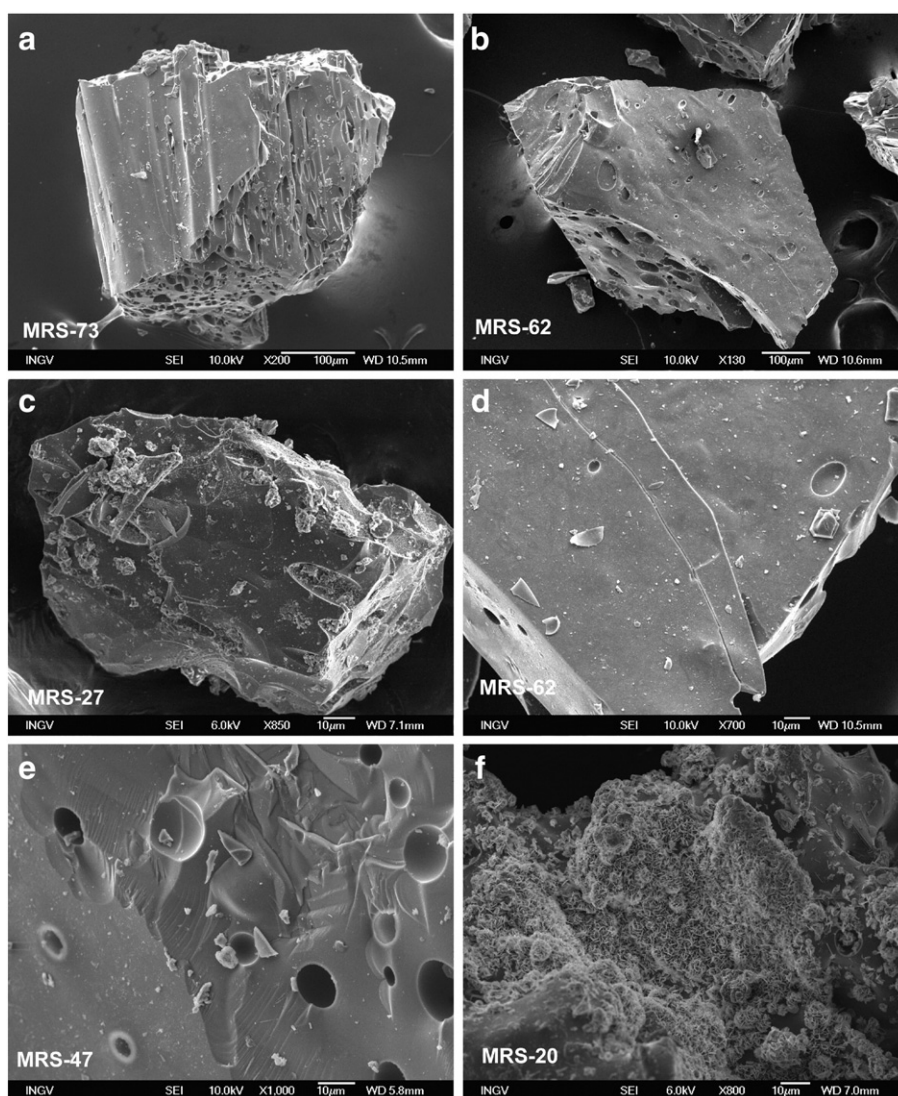


Fig. 3. Selected SEM photomicrographs showing the different morphologies of the CORO2 ash; the location of the samples is in Fig. 2. (a) Tube-like clast with stretched, elongated vesicles; (b) poorly vesiculated, smoothed clast with sub-circular bubbles; (c) clast with a blocky morphology and adhering particles (pitting) on its surface; (d) two cracks along a glassy fragment; (e) detail of a clast with concoidal to step-like ruptures; and (f) surface of a glassy clast with zeolites.

for Mrs-3/5 (1686–1443 yr BP, BP referred to 1950 A.D.), 1213–925 B.C. for Mrs-9/12 (3163–2875 yr BP), and 1289–718 B.C. for Mrs-33/36 (3239–2668 yr BP); within the cautionary limit of ± 0.2 ka of the ^{14}C age determination, the average years of these three sedimentary samples are 1.6 ka BP for Mrs-3/5, 3.0 ka BP for Mrs-9/12 and 3.0 ka BP for Mrs-33/36. These data suggest that the formation of the upper tephra is at about 3.0 ka BP and the lower one is older.

4. Discussion

4.1. Origin of the tephra layers

The collected data indicate that the TEPH01 and TEPH02 tephra layers record syn-eruptive flow (welded, poor sorting) and fall-like (loose, moderate sorting) deposition events (Fig. 2). This conclusion is also supported, according to the features of other submarine pyroclastic deposits (Head and Wilson, 2003), by the components of the tephra, which consist of 98 area% (TEPH1) and 100 area% (TEPH2) of volcanic, coarse to fine volcanic ash (Table 1), and by the occurrence of irregular, erosive surfaces at the top and bottom of the volcanic layers. According to Kano et al. (1996), the upward, general coarsening of clasts in our tephra may reflect the subaqueous nature of the pyroclastic eruptions,

whereas the local normal grading within contiguous layers of the same tephra indicates an intermittent-like activity and/or that the volcanic clasts quickly saturate while in the plume (Stewart and McPhie, 2004). The recognized erosive surfaces reflect the action of dense turbulent slurries that may erode the substratum on which they flow as well as the previously deposited pyroclastics (Head and Wilson, 2003).

The morphological features of the MS ash, i.e. tube-like and minor poorly smoothed and blocky clasts (Fig. 3), are consistent with those of fragments produced by magma fragmentation and minor magma-water interaction (White et al., 2003). The occurrence of stretched vesicles (Figs. 2, 3) may indicate, according to Polacci et al. (2003), high strain at the conduit walls before fragmentation and subsequent eruption, whereas the sub-circular vesicles are consistent with lower strains at the center of the conduit, where the velocity gradients are minimized.

In Fig. 4c, the TEPH01 and TEPH02 glasses are compared with those from the Tyrrhenian Sea bathyal plain (Paterne et al., 1988; Calanchi et al., 1994; Munno and Petrosino, 2004; Di Roberto et al., 2008) and from the Monticchio Lake section (Fig. 1b) (Wulf et al., 2004, 2008). These previous studies report that the glass composition of several moderate to high explosive subaerial eruptions occurred in mainland Italy, in the islands of the Tyrrhenian Sea, and in Sicily in the last

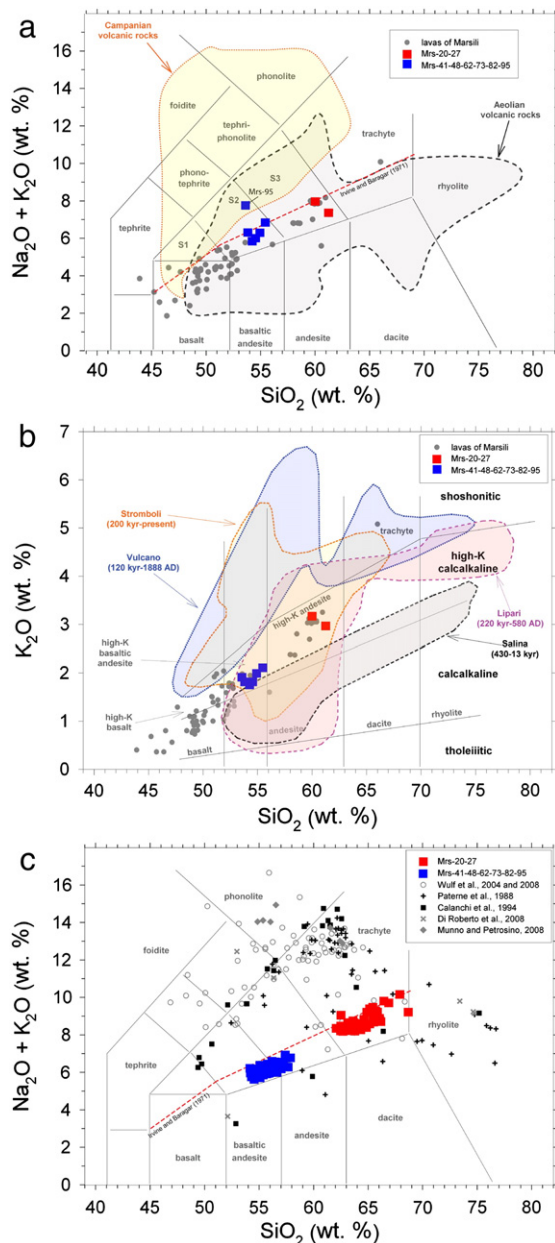


Fig. 4. a) TAS diagram reporting the bulk composition of TEPH01 and TEPH02, and of the MS lavas (data of MS lavas from Beccaluva et al., 1982; Trua et al., 2002, 2004, 2007); the fields of the Campanian and Aeolian volcanic rocks (location in Fig. 1b) are reported (data from Peccerillo, 2005; Santacroce et al., 2008); the boundary delimiting the alkaline and the sub-alkaline fields of Irvine and Baragar (1971) is also displayed. The anomalously high amount of alkali of the sample Mrs-95 from TEPH02 is due to contamination by sea-water brines (see text). b) K_2O vs. SiO_2 diagram showing the bulk composition of TEPH01 and TEPH02, MS lavas (same dataset of panel a), and the fields of the volcanoes of the Aeolian Islands Stromboli, Vulcano, Lipari and Salina (data from Peccerillo, 2005). The two tephra from COR02 lie on the trend of the MS lavas. c) TAS diagram of the TEPH01 and TEPH02 glasses plotted with all the distal tephra layers sampled in the Tyrrhenian Sea, San Gregorio Magno and Monticchio Lake.

100 ka. In Fig. 4c, TEPH02 has a glass composition different from that of the previously studied tephra, whereas TEPH01 slightly overlaps the samples from Mt. Etna (Sicily) eruptions at 16.5 and 18 ka, and the Pantelleria (Sicily Channel) eruption at 85 ka (Wulf et al., 2004, 2008). However, a provenance of the TEPH01 and TEPH02 ashes from Mt. Etna (Sicily) or Pantelleria can be excluded because the products of these volcanoes have a Na-alkaline affinity (Tanguy et al., 1997).

In Fig. 4a, the TEPH01 and TEPH02 compositions fall in the evolution trend of the MS lavas, overlap the trend of the Aeolian Islands (Southern Tyrrhenian Sea) and not that of the potassic undersaturated

and ultrapotassic saturated products of the Campanian volcanoes (Peccerillo, 2005). The signature of the Campanian rocks excludes a possible provenance of the COR02 tephra from these volcanoes (see also Fig. 4c).

The data of Fig. 4b confirm that both TEPH01 and TEPH02 samples align along the evolution trend of the MS lavas, and partly overlap the field of the Aeolian volcanoes of Stromboli, Lipari and Salina. These latter volcanoes are located 50 km south of MS (Fig. 1b). However, only Stromboli, Vulcano, and Lipari have erupted in the last 8–9 ka (De Astis et al., 2003), i.e. in a time span comparable to that of our age determinations. In the last 9 ka, Vulcano emitted shoshonitic to undersaturated magmas with a potassic affinity and Lipari erupted rhyolitic magmas (Gioncada et al., 2003). Therefore, we exclude a provenance of TEPH01 and TEPH02 from Vulcano and/or Lipari. At Stromboli, rocks of high-K calcalkaline affinity were emitted in the last 5 ka (Francalanci et al., 1993), but in the TIR2000 log (Fig. 1b) the only distal volcanic deposit referable to Stromboli is a <5 cm thick, 5 ka old layer with an extremely alkali-rich glass composition, i.e. $Na_2O + K_2O \approx 11$ wt.% (Table 3 and Fig. 7; Di Roberto et al., 2008). Therefore, we also rule out a provenance of the COR02 tephra from Stromboli.

In summary, we exclude that TEPH01 and TEPH02 represent products related to the activity of the Etna, Aeolian Islands and Campanian volcanoes. Stratigraphic data also indicate that the source area of the COR02 tephra cannot be a subaerial volcano. According to the data of Table 3 and Fig. 7, distal tephra layers in the Tyrrhenian Sea with thicknesses comparable to that of TEPH02 are present only at a depth of >3 m bsf (Campanian Ignimbrite and Tufo Verde of Mt. Epomeo from Campanian volcanoes) or very close to the Campanian coastline (79 A.D. eruption from Vesuvius) (Table 3 and Fig. 7). Nevertheless, the abovementioned three eruptions have geochemical features completely different from those of TEPH01 and TEPH02 (Fig. 4). The TIR2000 core is the closest section to the COR02 log (Fig. 1) and records only four distal tephra layers with thickness <5 cm (79 A.D. and AP from Vesuvius, GF from Lipari and LP from Salina) plus some volcanoclastic turbidites (Table 3 and Di Roberto et al., 2008) with geochemical features totally different from those of our samples (Fig. 4c). As a result, we conclude that the COR02 ashes record two submarine, explosive eruptions from MS. Taking into account our age determinations, these eruptions occurred at about 3 ka. The source area of the TEPH01 and TEPH02 ashes could be the central sector of MS, where cones lying on a flat surface have been recognized (Fig. 1d) (Ventura et al., 2013). The lack of deposits referable to TEPH01 and TEPH02 layers in the logs of the Marsili bathyal plain implies that these tephra have a limited dispersion; this could suggest a relatively low energy of the MS explosive eruptions.

In the SiO_2 vs. major and trace element plots (Fig. 5), the TEPH01 and TEPH02 samples well fit the trend of the MS lavas and fill the 52 wt.% < SiO_2 < 58 wt.% compositional gap previously recognized by Trua et al. (2002) in the MS succession. According to the results of the geochemical models by Trua et al. (2002), the evolution trend of the MS lavas (Fig. 5) reflects dominant fractional crystallization processes. Therefore, the TEPH01 latitic and trachytic magmas and the TEPH02 mugearites may derive from different degrees of fractional crystallization of a common parent basaltic source. IAB (Island Arc Basalts) and OIB-like (Oceanic Island Basalts) sources have been recognized at MS (Trua et al., 2007, 2010), with the OIB-like basalts erupted later. The trace element pattern of our less evolved samples (Mrs-73 and Mars-41, Fig. 6) is consistent with an OIB-like source, which has higher HFSE abundances with respect to the IAB, MS basalts. We remark, however, that the TEPH02 samples have higher Rb and K, possibly reflecting the crystallization of plagioclase (Bindeman and Davis, 2000).

4.2. Age constraints for the TEPH02 layer

The age and depth bsf of the tephra reported in Table 3 and our stratigraphic and geochronological data allow us to estimate the

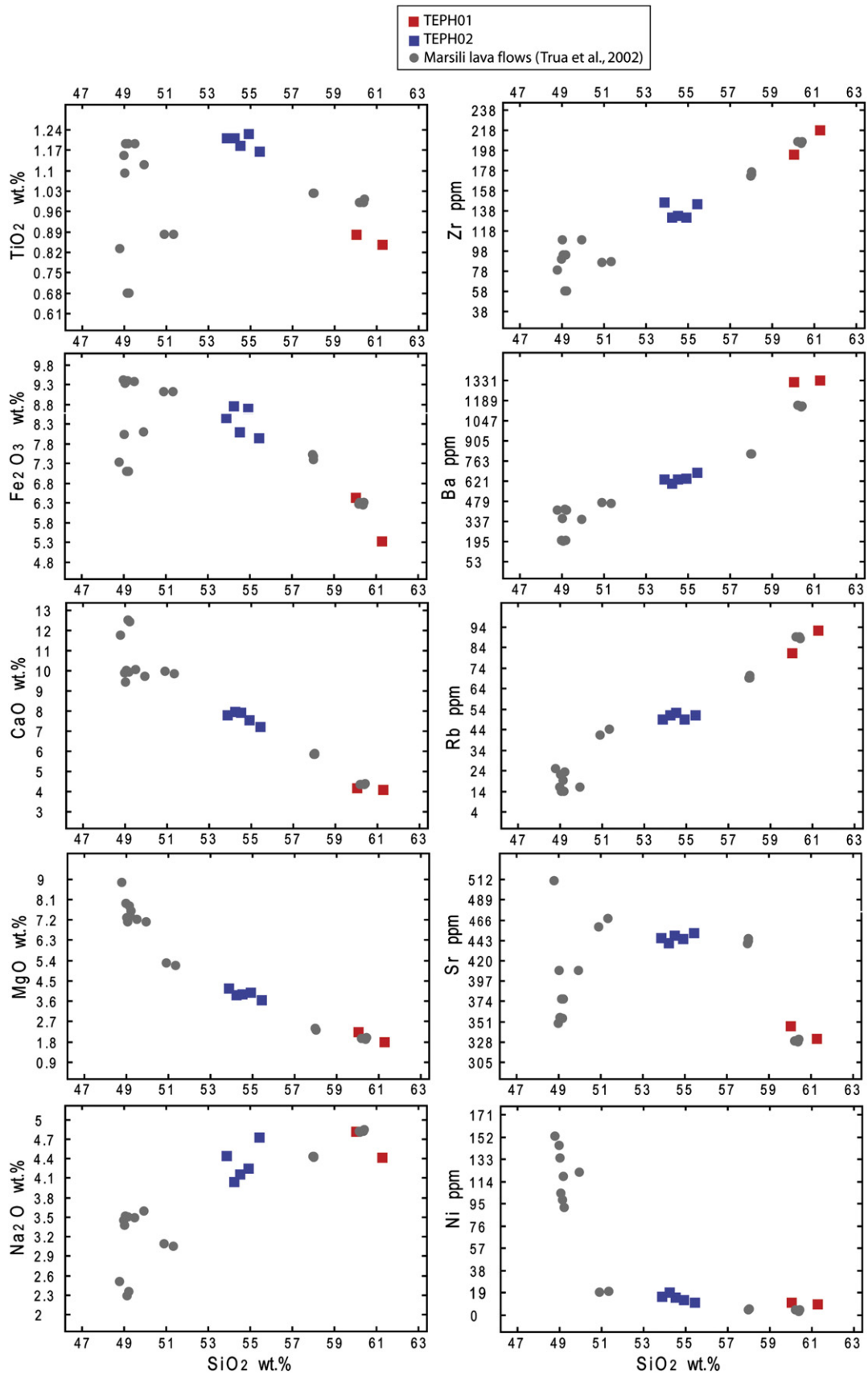


Fig. 5. SiO₂ (wt.%) vs selected major and trace elements of TEPH01 and TEPH02 samples (Table 2). The samples representative of the MS lavas (Trua et al., 2002) are reported for comparison.

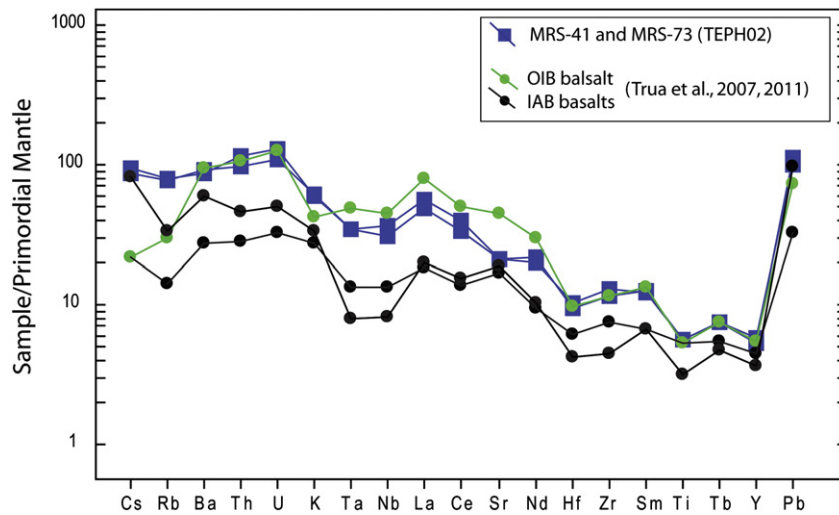


Fig. 6. Primordial mantle-normalized element variation diagrams (normalizing values from McDonough et al., 1992) of the less evolved TEPH02 samples (Table 2). Three representative samples of OIB-like and IAB basalts from MS are also reported for comparison (data from Trua et al., 2007, 2011).

sedimentation rate on and around MS in the last 70 ka. In the following, we exclude the C106 Tyrrhenian log from the rate estimation because of its proximity to the Campanian coast and volcanoes (Fig. 1b). The other six logs reported in Table 3 (KET8022, KET8003, KET8004, KET8011, C45 and TIR2000) give sedimentation rates between 0.07 and 0.17 mm/yr. However, the 0.17 mm/yr value calculated from the TIR2000 log is probably overestimated because of the significant thickness of volcanoclastic turbidites (Di Roberto et al., 2008). Therefore, we have determined a pelagic sedimentation rate in the Marsili basin between 0.07 and 0.13 mm/yr (average value of 0.1 mm/yr).

Excluding the erosion, the sedimentary layer above TEPH01 is 15 cm thick, and thus the resulting sedimentation rate is equal to 150 mm/3 ka, i.e. 0.05 mm/yr. This value approaches our lowest estimate of the sedimentation rate in the Marsili basin. Above TEPH02, the sedimentary layers reach 23 cm (15 + 8 cm) (Fig. 2). Using the above determined sedimentation rates of 0.05 mm/yr for MS and 0.1 mm/yr for the Marsili basin, we have calculated approximate ages of the TEPH02 tephra. In the absence of erosion, the calculation yields values between 4.6 ka and 2.3 ka. Therefore, we conclude that TEPH02 ash was emplaced in the last 5 ka.

Table 3

Main distal tephra layers in the shallower stratigraphic portions (<10 m bsf) and/or with an age <100 kyr identified in and around the Marsili basin (Southern Tyrrhenian Sea).

Reference	Core label	Tephra label	Depth bsf (cm)	Thickness (cm)	Eruption	Age (kyr)	Calculated sedimentation rate (mm/yr)
This study	COR02	Mrs-20 to -27	15	15	–	–	–
		Mrs-40 to -95	38	>60	–	–	–
Pateme et al. (1988)	KET8022	C2	87	<5	NYT	13	0.07
		C-13 (Y-5)	320	<15	CI	39	0.08
		C-18 (Y-7)	428	<5	TVE	60	0.07
	KET8003	E-2	130	<20	Pol	13	0.10
		Et-1 (Y-1)	170	<10	BVM	15	0.11
		C-13 (Y-5)	363	<20	CI	39	0.09
		C-18 (Y-7)	640	<5	TVE	60	0.11
	KET8004	C2	115	<5	NYT	13	0.09
		C-7 (Y-3)	274	<10	VRa	27	0.10
		C-13 (Y-5)	445	<40	CI	39	0.11
		C-16	560	<40	?	51*	0.11
		C-18 (Y-7)	640	<20	TVE	60	0.11
	KET8011	Et-1(Y-1)	116	<5	BVM	15	0.08
		C-13 (Y-5)	335	<15	CI	39	0.09
		C-17	420	<30	?	55*	0.08
		C-18 (Y-7)	480	<5	TVE	60	0.08
Di Roberto et al. (2008)	TIR2000	30 (E1)	30	<5	AP	3 ± 1	0.10
		50#	50	<5	SdL	5	0.10
		93	93	<5	GF	7	0.13
		417 (C-6)	417	<5	LP	24 ± 3	0.17
Munno and Petrosino (2007)	C106	A1	56	<60	AD79	2	0.28
		A2 (Y-3)	565	<15	VRa	30	0.19
	C45	B1	35	<10	AD79	2	0.17
		B2 (Y-3)	380	<5	VRa	30	0.13
		B3 (Y-5)	460	<5	CI	39	0.12

Tephra labels and ages are reported as in the original studies and possibly correlated to the major tephra markers of Tyrrhenian Sea according to Pateme et al., 1988 and Giaccio et al., 2008; abbreviations correspond to NYT – Neapolitan yellow tuff from Campi Flegrei (C2 in Giaccio et al., 2008), CI – Campanian Ignimbrite from Campi Flegrei (Y-5 or C-13 in Giaccio et al., 2008), TVE – Tufo Verde Mt. Epomeo from Ischia (Y-7 or C-18 in Giaccio et al., 2008); BVM – Biancavilla-Montalto Ignimbrite from Etna (Y-1 or Et-1 in Giaccio et al., 2008), VRa – eruption from Campi Flegrei (Y-3 or C-7 in Giaccio et al., 2008), Pol – Pollara eruption from Salina, LP – Lower Pollara from Salina, GF – Gabelotto-Fiumebianco eruption from Lipari; AP – Avellino and Pollena sub-Plinian eruptions; AD79: Pompei eruption from Vesuvio, SdL: Secche di Lazzaro from Stromboli.

* Age inferred from stratigraphy.

Volcaniclastic turbidite with a glass component <90% but identifiable as a known eruption.

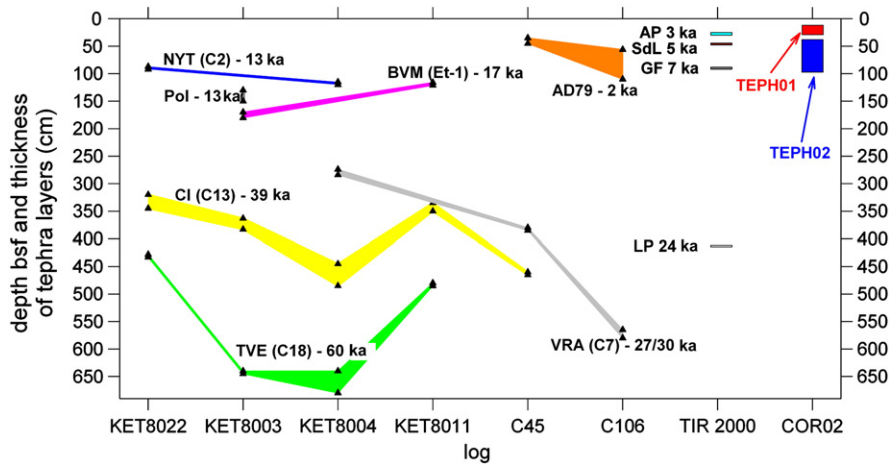


Fig. 7. Stratigraphic data (depth bsf) and age of the main tephra layers found in the Tyrrhenian Sea around MS compared with those of TEPH01 and TEPH02; the labels, data and references are summarized in Table 3. See Fig. 1b for the location of these cores.

5. Conclusions

The main conclusions of this study can be summarized as follows:

- (1) The two studied tephra record two MS submarine explosive eruptions that produced fall and flow deposits in historical times.
- (2) According to ^{14}C age determinations, the upper tephra was emplaced at about 3.0 ka BP. On the basis of sedimentation rate calculations and assuming absence of erosion processes, the lower tephra was emplaced at about 5.0 ka BP.
- (3) The location of the COR02 gravity core on MS suggests that source areas were located in the central sector of the seamount, where numerous pyroclastic cones lie on a relatively flat surface.
- (4) The results of this study, along with the geophysical and geochemical evidence of intra-seamount seismicity and active hydrothermal/degassing processes, point out that MS is still active and can erupt explosively. As a result, MS should be monitored and the hazard(s) related to explosive eruptions evaluated. In light of our data, the active volcanoes of the Tyrrhenian Sea now include Stromboli, Vulcano, Lipari, Panarea, and Marsili Seamount.

Further studies on the MS tephra will be carried out to (a) unravel how a very low bubble content like that measured here is produced during a submarine explosive eruption, and (b) how it better constrains the magma differentiation mechanism(s). Finally, this study provides the first evidence of a deep, explosive submarine activity in the Mediterranean Sea.

Acknowledgments

We dedicate this study to Bruno Di Sabatino, who passed away some years ago at the beginning of the research activities on the Marsili Seamount. We thank the three anonymous GR reviewers and the associated editor Inna Safonova for the useful, constructive comments. The authors thank Carmine Lubritto for ^{14}C AMS analyses. This study was supported by the Eurobuilding Spa, the University G. d'Annunzio, the MIUR via the PRIN project "Experimental determination of the glass-forming ability (GFA), nucleation and crystallization of natural silicate melts" awarded to G. Iezzi. F. Vetere is supported by a Marie Curie fellowship SolVoM #297880. S. Mollo is supported by ERC 611 Starting Grant GLASS (#259256). This study has been carried out within the IYPE-UNESCO accredited 'Creep' project awarded to G. Ventura.

References

- Beccaluva, L., Rossi, P.L., Serri, G., 1982. Neogene to recent volcanism of the Southern Tyrrhenian–Sicilian area: implications for the geodynamic evolution of the Calabrian arc. *Earth Evolutionary Sciences* 3, 222–238.
- Bindeman, I., Davis, A., 2000. Trace element partitioning between plagioclase and melt: investigation of dopant influence on partition behaviour. *Geochimica et Cosmochimica Acta* 64, 2863–2878.
- Calanchi, N., Gasparotto, G., Romagnoli, C., 1994. Glass chemistry in volcanoclastic sediments of ODP Leg 107, Site 650, sedimentary sequence: provenance and chronological implications. *Journal of Volcanology and Geothermal Research* 60, 59–85.
- Caratori Tontini, F., Cocchi, L., Muccini, F., Carmisciano, C., Marani, M., Bonatti, E., Ligi, M., Boschi, E., 2010. Potential-field modeling of collapse-prone submarine volcanoes in the Southern Tyrrhenian Sea (Italy). *Geophysical Research Letters* 37, L03305.
- Caso, C., Signanini, P., De Santis, A., Favali, P., Iezzi, G., Marani, M.P., Paltrinieri, D., Rainone, M.D., Di Sabatino, B., 2010. Submarine geothermal systems in Southern Tyrrhenian Sea as future energy resource: the example of Marsili seamount. *Proceedings World Geothermal Congress 2010, Bali, Indonesia*, pp. 1–9.
- Cocchi, L., Caratori, Tontini, F., Muccini, F., Marani, M.P., Bortoluzzi, G., Carmisciano, C., 2009. Chronology of the transition from a spreading ridge to an accretional seamount in the Marsili backarc basin (Tyrrhenian Sea). *Terra Nova* 21, 369–374.
- D'Alessandro, A., D'Anna, G., Luzio, D., Mangano, G., 2009. The INGV's new OBS/H: analysis of the signals recorded at the Marsili submarine volcano. *Journal of Volcanology and Geothermal Research* 183, 17–29.
- De Astis, G., Ventura, G., Vilardo, G., 2003. Geodynamic significance of the Aeolian volcanism (Southern Tyrrhenian Sea, Italy) in light of structural, seismological, and geochemical data. *Tectonics* 22. <http://dx.doi.org/10.1029/2003TC001506>.
- De Ritis, R., Ventura, G., Chiappini, M., Carluccio, R., Von Frese, R., 2010. Regional magnetic and gravity anomaly correlations of the Southern Tyrrhenian Sea. *Physics of the Earth and Planetary Interiors* 181, 27–41. <http://dx.doi.org/10.1016/j.pepi.2010.04.003>.
- Di Roberto, A., Rosi, M., Bertagnini, A., Marani, M.P., Gamberi, F., Del Principe, A., 2008. Deep water gravity core from the Marsili Basin (Tyrrhenian Sea) records Pleistocene–Holocene explosive events and instabilities of the Aeolian Island Archipelago (Italy). *Journal of Volcanology and Geothermal Research* 177, 133–144.
- Francalanci, L., Taylor, S.R., McCulloch, M.T., Woodhead, J.D., 1993. Geochemical and isotopic variations in the calc-alkaline rocks of Aeolian arc, Southern Tyrrhenian Sea, Italy: constraints on magma genesis. *Contributions to Mineralogy and Petrology* 113, 300–313.
- Giaccio, B., Isaia, R., Fedele, F., Di Canzio, E., Hoffecker, J., Ronchitelli, A., Sinitsyn, A., Anikovich, M., Lisitsyn, S., Popov, V., 2008. The Campanian Ignimbrite and Codola tephra layers: Two temporal/stratigraphic markers for the Early Upper Palaeolithic in southern Italy and eastern Europe. *Journal of Volcanology and Geothermal Research* 177, 208–226. <http://dx.doi.org/10.1016/j.jvolgeores.2007.10.007>.
- Gioncada, A., Mazzuoli, R., Bisson, M., Pareschi, M.T., 2003. Petrology of volcanic products younger than 42 ka on the Lipari–Vulcano complex (Aeolian Islands, Italy): An example of volcanism controlled by tectonics. *Journal of Volcanology and Geothermal Research* 122, 191–220.
- Head, J.W., Wilson, L., 2003. Deep submarine pyroclastic eruptions: theory and predicted landforms and deposits. *Journal of Volcanology and Geothermal Research* 121, 155–193.
- Hughes, K.A., Baillie, M.G.L., Bard, E., Bayliss, A., Beck, J.W., Bertrand, C., Blackwell, P.G., Buck, C.E., Burr, G., Cutler, K.B., Damon, P.E., Edwards, R.L., Fairbanks, R.G., Friedrich, M., Guilderson, T.P., Kromer, B., McCormac, F.G., Manning, S., Bronk, R.C., Reimer, P.J., Reimer, R.W., Remmele, S., Southon, J.R., Stuiver, M., Talamo, S., Taylor, F.W., van der Plicht, J., Weyhenmeyer, C.E., 2004. *Radiocarbon* 46, 1059–1086.
- Iezzi, G., Mollo, S., Ventura, G., Cavallo, A., Romano, C., 2008. Experimental solidification of anhydrous latic and trachytic melts at different cooling rates: the role of nucleation kinetics. *Chemical Geology* 253, 91–101.
- Iezzi, G., Mollo, S., Torresi, G., Ventura, G., Cavallo, A., Scarlato, P., 2011. Experimental solidification of an andesitic melt by cooling. *Chemical Geology* 253, 91–101.

- Irvine, T.N., Baragar, W.R., 1971. A guide to the chemical classification of the common igneous rocks. *Canadian Journal of Earth Sciences* 8, 523–548.
- Kano, K., Yamamoto, T., Ono, K., 1996. Subaqueous eruption and emplacement of the Shinjima Pumice, Shinjima (Mooshima) Island, Kagoshima Bay, SW Japan. *Journal of Volcanology and Geothermal Research* 71, 187–206.
- Keller, J., Leiber, J., 1974. Chemical composition, trace elements and norm of volcanic lapilli of sediment core M22_103, South Tyrrhenian Sea. In: Keller, J., Leiber, J. (Eds.), *Sedimente, Tephra-Lagen und Basalte der südtyrrhenischen Tiefsee-Ebene im Bereich des Marsili-Seeberges. Meteor Forschungsergebnisse, Deutsche Forschungsgemeinschaft, Reihe C Geologie und Geophysik*, C19. Gebrüder Bornträger, Berlin, Stuttgart, pp. 62–76.
- Lanzafame, G., Mollo, S., Iezzi, G., Ferlito, C., Ventura, G., 2013. Unravelling the solidification path of a pahoehoe “cicirara” lava from Mount Etna volcano. *Bulletin of Volcanology* 75, 1–16.
- Le Bas, M.J., Le Maitre, R.W., Streckeisen, A., Zanettin, B., 1986. A chemical classification of volcanic rocks based on the total alkali–silica diagram. *Journal of Petrology* 27, 745–750.
- Lupton, J., De Ronde, C., Sprovieri, M., Baker, E.T., Bruno, P.P., Italiano, F., Walker, S., Faure, K., Leybourne, M., Britten, K., Greene, R., 2011. Active hydrothermal discharge on the submarine Aeolian Arc. *Journal of Geophysical Research B: Solid Earth* 116, B02102.
- Malinverno, A., Ryan, W.B.F., 1986. Extension in the Tyrrhenian Sea and shortening in the Apennines as result of arc migration driven by sinking of the lithosphere. *Tectonics* 5, 227–245.
- Marani, M., Trua, T., 2002. Thermal constriction and slab tearing at the origin of a super-inflated spreading ridge: the Marsili volcano (Tyrrhenian Sea). *Journal of Geophysical Research* 107. <http://dx.doi.org/10.1029/2001JB000285>.
- McDonough, W.F., Sun, S.S., Ringwood, A.E., Jagoutz, E., Hofmann, A.W., 1992. K, Rb and Cs in the earth and moon and the evolution of the earth's mantle. *Geochimica et Cosmochimica Acta* 56, 1001–1012.
- Mollo, S., Scarlato, P., Lanzafame, G., Ferlito, C., 2013. Deciphering lava flow post-eruption differentiation processes by means of geochemical and isotopic variations: a case study from Mt. Etna volcano. *Lithos* 162–163, 115–127.
- Munno, R., Petrosino, P., 2004. New constraints on the occurrence of Y-3 Upper Pleistocene tephra marker layer in the Tyrrhenian Sea. *Il Quaternario* 17, 11–20.
- Munno, R., Petrosino, P., 2007. The late Quaternary tephrostratigraphical record of the San Gregorio Magno basin (Southern Italy). *Journal of Quaternary Science* 22, 247–266.
- Nicolosi, I., Speranza, F., Chiappino, M., 2006. Ultrafast oceanic spreading of the Marisili basin, Southern Tyrrhenian Sea: evidence from magnetic anomaly analysis. *Geology* 34, 717–720.
- Paterne, M., Guichard, F., Labeyrie, J., 1988. Explosive activity of the South Italian volcanoes during the past 80,000 years as determined by marine tephrochronology. *Journal of Volcanology and Geothermal Research* 34, 153–172.
- Peccherillo, A., 2005. *Plio-quaternary Volcanism in Italy*. Springer, Berlin 356.
- Polacci, M., Pioli, L., Rosi, M., 2003. The Plinian phase of the Campanian Ignimbrite eruption (phlegrean fields, Italy): Evidence from density measurements and textural characterization of pumice. *Bulletin of Volcanology* 65, 418–432.
- Rosenbaum, G., Lister, G.S., 2004. Neogene and Quaternary rollback evolution of the Tyrrhenian Sea, the Apennines, and the Sicilian Maghrebides. *Tectonics* 23, 1–17.
- Santacroce, R., Cioni, R., Marianelli, P., Sbrana, A., Sulpizio, R., Zanchetta, G., Donahue, D.J., Joron, J.L., 2008. Age and whole rock–glass compositions of proximal pyroclastics from the major explosive eruptions of Somma–Vesuvius: a review as a tool for distal tephrostratigraphy. *Journal of Volcanology and Geothermal Research* 177, 1–18.
- Selli, R., Lucchini, F., Rossi, P., Savelli, C., Del Monte, M., 1977. Dati geologici, petrochimici, e radiometrici sui vulcani centro-tirrenici. *Giornale di Geologia* 2, 221–246.
- Siani, G., Paterne, M., Michel, E., Sulpizio, R., Sbrana, A., Arnold, M., Haddad, G., 2001. Mediterranean sea surface radiocarbon reservoir age changes since the Last Glacial Maximum. *Science* 294, 1917–1920.
- Stewart, A.L., McPhie, J., 2004. An Upper Pliocene coarse pumice breccia generated by a shallow submarine explosive eruption, Milos, Greece. *Bulletin of Volcanology* 66, 15–28. <http://dx.doi.org/10.1007/s00445-003-0292-z>.
- Tanguy, J.C., Condomines, M., Kieffer, G., 1997. Evolution of the Mount Etna magma: constraints on the present feeding system and eruptive mechanism. *Journal of Volcanology and Geothermal Research* 75, 221–250.
- Terrasi, F., Rogalla, D., De Cesare, N., D'Onofrio, A., Lubritto, C., Marzaioli, F., Passariello, I., Rubino, M., Sabbarese, C., Casa, G., Palmieri, A., Gialanella, L., Imbriani, G., Roca, V., Romano, M., Sundquist, M., Loger, R., 2007. A new AMS facility in Caserta/Italy. *Nuclear Instruments and Methods in Physics Research Section B: Beam Interactions with Materials and Atoms* 259, 14–17.
- Trua, T., Serri, G., Marani, M.P., Renzulli, A., Gamberi, F., 2002. Volcanological and petrological evolution of Marsili seamount (Southern Tyrrhenian Sea). *Journal of Volcanology and Geothermal Research* 114, 441–464.
- Trua, T., Serri, G., Marani, M.P., Rossi, P.L., Gamberi, F., Renzulli, A., 2004. Mantle domains beneath the Southern Tyrrhenian: constraints from recent seafloor sampling and dynamic implications. *Periodico di Mineralogia* 73, 53–73.
- Trua, T., Serri, G., Rossi, P.L., 2005. Coexistence of IAB-type and OIB-type magmas in the Southern Tyrrhenian back-arc basin: evidence from recent seafloor sampling and geodynamic implications. In: Marani, M.P., Gamberi, F., Bonatti, E. (Eds.), *From Seafloor to Deep Mantle: Architecture of the Tyrrhenian Backarc Basin*. *Memorie Descrittive della Carta Geologica d'Italia*, pp. 83–96.
- Trua, T., Serri, G., Marani, M.P., 2007. Geochemical features and geodynamic significance of the Southern Tyrrhenian backarc basin. In: Beccaluva, L., Bianchini, G., Wilson, M. (Eds.), *Cenozoic Volcanism in the Mediterranean Area*. *The Geological Society of America, Special Paper*, 418, pp. 221–233.
- Trua, T., Clocchiatti, R., Schiano, P., Ottolini, L., Marani, M., 2010. The heterogeneous nature of the Southern Tyrrhenian mantle: evidence from olivine-hosted melt inclusions from back-arc magmas of the Marsili seamount. *Lithos* 118, 1–16. <http://dx.doi.org/10.1016/j.lithos.2010.03.008>.
- Trua, T., Marani, M.P., Gamberi, F., 2011. Magmatic evidence for African mantle propagation into the Southern Tyrrhenian backarc region. In: Beccaluva, L., Bianchini, G., Wilson, M. (Eds.), *Volcanism and Evolution of the African Lithosphere*. *The Geological Society of America, Special Paper*, 478, pp. 307–331.
- Ventura, G., Milano, G., Passaro, S., Sprovieri, M., 2013. The Marsili Ridge (Southern Tyrrhenian Sea, Italy): an island-arc volcanic complex emplaced on a ‘relict’ back-arc basin. *Earth-Science Reviews* 116, 85–94.
- White, J.D.L., Smellie, J.L., Clague, D.A., 2003. Introduction: a deductive outline and topical overview of subaqueous explosive volcanism. In: White, J.D.L., Smellie, J., Clague, D.A. (Eds.), *Explosive Subaqueous Volcanism*. *AGU Geophysical Monograph*, 140. American Geophysical Union, Washington, DC, pp. 1–23.
- Wulf, S., Kraml, M., Keller, J., Negendank, J.F.W., 2004. Tephrochronology of the 100 ka lacustrine sediment record of Lago Grande di Monticchio (Southern Italy). *Quaternary International* 122, 7–30.
- Wulf, S., Kraml, M., Keller, J., 2008. Towards a detailed distal tephrostratigraphy in the Central Mediterranean: the last 20,000 yrs record of Lago Grande di Monticchio. *Journal of Volcanology and Geothermal Research* 177, 118–132.